LA-UR-12-00159

Approved for public release;
distribution is unlimited.

Title: Cross Section Data Benchmarking using Automated Criticality Benchmarks in MCNP6 and Partisn

Author(s):
Eric Relson
Jeremy Lloyd Conlin
D. Kent Parson

Intended for:
2012 ANS Annual Meeting
Chicago, IL
June 24–28, 2012

Cross Section Data Benchmarking using Automated Criticality Benchmarks in MCNP6 and Partisn

Eric Relson[1,2], Jeremy Lloyd Conlin[1], D. Kent Parsons[1]

[1]*Los Alamos National Laboratory, PO Box 1663, Los Alamos, NM, 87545, USA*
[2]*Department of Engineering Physics, University of Wisconsin-Madison, Madison, WI, 53706*
relson@wisc.edu, jlconlin@lanl.gov, dkp@lanl.gov

INTRODUCTION

Nuclear transport codes use reaction cross-section data to determine all manner of particle interactions. These data typically take the form of probabilities at specific particle energies. For practicality and efficiency reasons, nuclear codes use various multigroup approximations where cross section data are combined into discrete values for a set of energy groups using flux weighting [1]. When modifications are made to the cross-section data or the collapsing approach, the results of calculations using these data can change. Evaluating changes of this sort requires running test cases and evaluating the results for changes and trends. This work aims to address the need for more extensive testing of changes and improvements to multigroup neutron cross sections for criticality problems.

A large number of test problems are needed to span the range of energies and materials of interest – but automation is the only feasible method of managing these tests and reevaluations. Tools were developed to run the Monte Carlo code MCNP6 [2] and the deterministic code Partisn [3], as well as to create Partisn inputs from MCNP6 input files. These tools then parse the results from each code and present trends and changes between different data sets. The primary metric used is k_{eff}, and the codes are compared with each other and with the experimental benchmark measurements of k_{eff}.

BENCHMARK SETUP AND SCOPE

717 criticality benchmark problems were taken from the International Handbook of Evaluated Criticality Safety Benchmark Experiments [4] (ICSBEP). These benchmarks are all real world experiments with inferred values ("measurements") of k_{eff}. The benchmarks selected from ICSBEP have fairly simple geometries featuring various fissile materials reflected by common reflectors, and with thermal, intermediate, fast or mixed neutron spectra. The selection of benchmarks is based on two overlapping evaluations – the 119 benchmarks in the "Expanded Criticality Validation Suite for MCNP" [5], and a suite of 662 benchmarks selected by Kahler, et al. [6] for cross section data testing.

MCNP6 input decks were already available for the selected 717 benchmark cases, but corresponding Partisn input files were not available. Using newly developed conversion scripts, 405 of the MCNP6 inputs were successfully converted into Partisn inputs.

The cross section data used for the Partisn calculations is a 30 group library collapsed from the 618 group library, MENDF70x, used at Los Alamos National Lab (LANL), and does not include upscattering. The neutron flux used to collapse the cross section into 618 groups is typical of a fast metal critical assembly. Both the multigroup and the continuous-energy cross sections were processed with NJOY and come from the ENDF/B-VII.0 release of the data.

METHOD

The two codes were automated using python scripts to generate sets of shell scripts which sequentially run problems on clusters. The resulting outputs are parsed with additional scripts, and the parsed information from each code is combined together for comparison.

The bulk of the scripting support for this work focused on automating the conversion of MCNP6 input files to Partisn input files. This provides flexibility for adding large numbers of new benchmark problems to the test suite.

The primary challenge in this conversion is that the two codes use different geometry definitions. MCNP6 defines geometry as a set of cells – volumes defined by surfaces and Boolean logic. Each surface in a cell definition has a 'sense,' which define which side of the surface the cell exists on. For example, in the case of a planar surface, the sense denotes which half-space the cell volume is in. On the other hand, Partisn uses structured meshing.

In order to determine the materials for the Partisn mesh, the MCNP6 geometry information needs to be matched to the structured mesh. To do this conversion, the developed script first uses the MCNP6 surfaces to determine a structured mesh for Partisn that does not have any mesh voxels that contain parts of multiple cells. For each voxel in the Partisn mesh, we need to know the MCNP6 cell containing it, in order to assign the voxel's material.

The script calculates a given voxel's center point. For a given cell in the problem, the cell's defining surfaces are each evaluated with respect to voxel center point. These evaluations give a list of Boolean values. (e.g. for a planar surface, true, the point is in the half-space defined by the surface; false, it is not in the half-space.) After evaluating each surface, we now have a series Boolean values with logical AND and OR operators, and parentheses – this Boolean statement relates the given cell and voxel. (Geometrically, AND and OR represent intersections and unions, respectively.) We then evaluate these Booleans in a manner akin to the 'order of operations' used in algebraic math with an iterative three step process: (1) evaluate AND; (2) evaluate OR; (3) remove parentheses around single Boolean values; and repeat as needed until our Boolean statement is condensed to a single Boolean value giving the relation between the voxel center point and the MCNP6. If this value is false, we repeat the process with another cell until the containing cell is found, and in turn repeat until all voxels have been assigned a material.

In order for this conversion method to work, the MCNP6 geometry must be exactly definable with a structured mesh. Concentric spheres and cylinders, and planar geometries (x-y-z) fit this criterion, while adjacent cylinders or spheres cannot be modeled with a structured mesh in Partisn. Fortunately, the majority of the benchmarks of interest are compatible with both codes' geometry definitions and can be exactly modeled. Of the 405 benchmarks that were convertible with this method, 275 were spherical cases, 123 were cylindrical (r-z) cases, and 7 were x-y-z geometries.

A second method of creating Partisn inputs using new functionality being added to MCNP6 is also supported by the automated testing suite. This functionality is still under development. This method overlays a structured mesh on the MCNP6 geometry, and then uses point sampling to create a smeared material, structured mesh that Partisn can use. The point sampling approach can approximate the more complex geometries that the developed conversion script cannot handle, but provides less flexibility when creating the Partisn input files. Currently, this capability is only automated for the same 405 benchmark configurations where the geometry can be mapped exactly to a structured mesh.

RESULTS

Benchmarks for highly enriched uranium metal with fast neutron spectrum, for example, are considered an ideal application of the collapsing methods used to get the 30 group cross section data used in Partisn. However, for the initial test suite work, these cross sections were applied to all manner of criticality problems (thermal and fast, fissile metal or in solution). In part, analysis looked for trends that were independent of the mismatch between cross section data and system. An example of such trends is correlation between k_{eff} values and the relative quantities of reflecting and fissile material. Some of these benchmarks are presented here as an example of the test suite results.

Figure 1 shows the discrepancy between the k_{eff} values calculated by Partisn and MCNP6 and the values inferred from experiments ($k_{eff,calculated}$ - $k_{eff,measured}$). Three benchmarks, each with several individual experiment configurations are shown in Figure 1, with benchmarks delineated by the dashed line. The benchmarks in Figure 1 are referred to in the ICSBEP handbook as HEU-MET-FAST-058, -066, and -077. [4] We will abbreviate these as HMF58, HMF66 and HMF77. The ordering of configurations in Figure 1 matches the ordering in the ICSBEP handbook.

The HMF58, HMF66 and HMF77 benchmarks are all part of the *Nimbus* experiments performed at Lawrence Livermore National Lab (LLNL) circa 1960. [4] The HMF58 benchmarks are HEU spheres reflected by Be. The HMF66 configurations are spherical highly enriched uranium (HEU) shells with internal and external Be shells to moderate and reflect, respectively. The HMF77 configurations are spherical HEU shells reflected by larger radius beryllium metal shells. The measured values for k_{eff} are 1 for all HMF58 and HM66 configurations. For the HMF77 configurations, k_{eff} ranges from 0.9994 to 1.

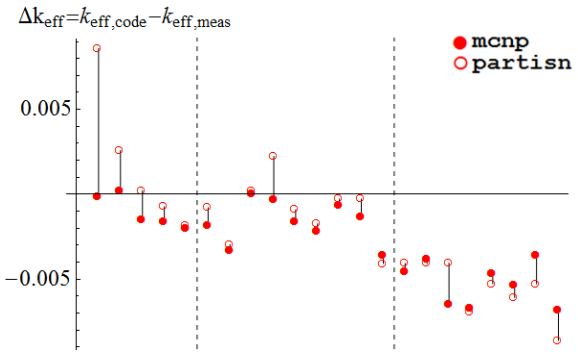

Fig. 1. Comparison of k_{eff} discrepancies for spherical fast spectrum highly enriched uranium and Be configuration of various radii. Dashed lines separate, from left to right, the HEU-MET-FAST-058, -066, and -077 benchmarks. [4] For MCNP values, all errors are ≤ 0.00011.

The best agreement with measured values is seen for the HMF66 configurations. For all but one of the

HMF58 and HMF66 configurations, Partisn overestimates k_{eff}. For both codes, and all three benchmarks, there appears to be a correlation between higher fissile mass (and less reflector/moderator mass) and lower estimates of k_{eff}.

We next highlight two benchmark sets with more exotic materials. These benchmarks are based on the *Falstaff* experiments performed at LLNL in the late 1950's. [4] These experiments feature stainless steel spherical vessels containing aqueous ^{233}U uranyl fluoride solutions reflected by Be or CH_2. Experiments where both reflecting materials are used simultaneously were not included in the test suite. The two sets are distinguished by neutron energy spectra that are predominantly intermediate (0.625 eV – 100 keV) or thermal (< 0.625 eV). For the ^{233}U benchmarks, the measured k_{eff} is given to be 1. The benchmarks in Figures 2 and 3 are referred to in the ICSBEP handbook as U233-SOL-INTER-001 and U233-SOL-THERM-015. [4]

Figure 2 shows the discrepancies from each code for the intermediate spectrum benchmarks. Figure 3 shows the same discrepancies for the thermal spectra benchmarks. Both plots order the data points by the listings in the ICSBEP handbook. We note that for these cases, the discrepancies are generally greater than seen in Figure 1. This is expected, as the uranyl fluoride benchmarks are not fast metal systems.

In both Figures 2 and 3, we see that MCNP6 always underestimates k_{eff}. The k_{eff} values from Partisn are usually larger than the MCNP6 values. This observation matches the expected behavior. Only downscattering occurs in the Partisn calculations – the lack of upscattering leads to softening of the neutron spectrum, and in turn, a greater multiplication of neutrons via fission, and a higher k_{eff}.

The benchmark cases are grouped by the uranyl fluoride solution used – seven different uranyl fluoride concentrations were used in the Falstaff experiments. Groupings by these concentrations are delineated by dashed lines in Figures 2 and 3. For each solution, several container sizes were used, with correspondingly varying reflector thicknesses.

It is not apparent why the outlier of the intermediate spectrum benchmarks for Partisn overestimates k_{eff} by 0.0434, while the MCNP6 result for the same configuration is similar to other cases.

The last six thermal spectrum cases are those with the lowest concentration of uranyl fluoride. These cases also include the only three benchmarks where Partisn gave a lower k_{eff} value.

In general, the difference between Partisn and MCNP6 values of k_{eff} decreases from left to right within each group of experiments in Figures 2 and 3. This corresponds with increasing solution volume and decreasing reflector thickness.

Particularly in the thermal cases (Figure 3), a similar trend is seen for decreasing estimates of k_{eff} from both codes. This decrease is greater for the Partisn cases.

Other benchmarks featuring ^{233}U in solution with other elements show less deviation from $k_{eff} = 1$ for both codes. This suggests that there may be cross section data inaccuracies with ^{19}F isotopes.

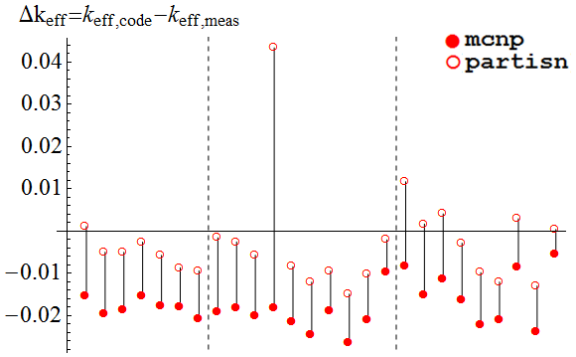

Fig. 2. Comparison of k_{eff} discrepancies for intermediate spectrum, beryllium reflected, aqueous uranyl fluoride (^{233}U) spheres with varying concentrations and solution/reflector radii. Dashed lines separate different concentrations of uranyl fluoride. For MCNP values, all errors are ≤ 0.00016.

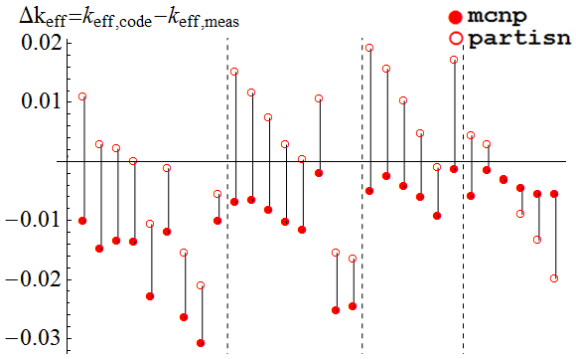

Fig. 3. Comparison of k_{eff} discrepancies for thermal spectrum, beryllium reflected, aqueous uranyl fluoride (^{233}U) spheres with varying concentrations and solution/reflector radii. Dashed lines separate different concentrations of uranyl fluoride. For MCNP values, all errors are ≤ 0.00016.

CONCLUSIONS & FUTURE WORK

The initial focus of future work is to continue to improve the automated testing capabilities. The stated goal of comparing old and new results has not been implemented, and initial assessment of typical changes between cross section data revisions needs to be done.

In comparing Partisn and MCNP results, large discrepancies were often correlated with expected contributions of the multigroup collapsing process, e.g. lack of upscattering, and collapsing the cross sections with a neutron spectrum ideal for fast metal systems. Running Partisn with the upscattering included would quantify this contribution.

Furthermore, the scope of this testing suite can be improved by including multiple sets of cross section data, each with different assumptions made during data condensation. Which sets of cross section data to include might be best determined by comparisons between the test suite results for previous data sets.

ACKNOWLEDGEMENTS

Thanks to Larry Cox at LANL for support with using the work-in-progress MCNP-to-Partisn functionality being added to MCNP6.

REFERENCES

1. G.I. BELL and S. GLASSTONE, Nuclear Reactor Theory, Ban Nostrand, Princeton, N. J. (1970).
2. T. GOORLEY, M. JAMES, T. BOOTH, F. BROWN, J. BULL, L.J. COX, J. DURKEE, J. ELSON, M. FENSIN, R.A. FORSTER, J. HENDRICKS, H.G. HUGES, R. JOHNS, B. KIEDROWSKI, R. MARTZ, S. MASHNIK, G. McKINNEY, D. PELOWITZ, R. PRAEL, J. SWEEZY, L. WATERS, T. WILCOX, T. ZUKAITIS, "Initial MCNP6 Release Overview", submitted to *Nuclear Technology*, LA-UR-11-05198 (December 2011).
3. R.E. ALCOUFFE, R.S. BAKER, J.A. DAHL, S.A. TURNER, R.C. WARD, "PARTISN: A Time-Dependent, Parallel Neutral Particle Transport Code System." LA-UR-08-07258 (November 2008).
4. NUCLEAR ENERGY AGENCY – NUCLEAR SCIENCE COMMITTEE, "International Handbook of Evaluated Criticality Safety Benchmark Experiments." September 2010 Edition, NEA/NSC/DOC(95)03 (2010).
5. R.D. MOSTELLER, "An Expanded Criticality Validation Suite for MCNP." *Trans. ANS*, **104**, pgs. 453-455 (June 2011).
6. A.C. KAHLER, R.E. MacFARLANE, R.D. MOSTELLER, B.C. KIEDROWSKI, S.C. FRANKLE, M.B. CHADWICK, R.D. McKNIGHT, R.M. LELL, G. PALMIOTTI, H. HIRUTA, M. HERMAN, R. ARCILLA, S.F. MUGHABGHAB, J.C. SUBLET, A. TRKOV, T.H. TRUMBULL, M. DUNN, "ENDF/B-VII.1 Neutron Cross Section Data Testing with Critical Assembly Benchmarks and Reactor Experiments." *Nuclear Data Sheets* **112** pgs. 2997-3036 (2011).